Uncertainty Quantification of High-Velocity Impact Fracture in Fiber-Reinforced Composites Using a Robust Stochastic Sampling Approach

Uncertainty Quantification of High-Velocity Impact Fracture in Fiber-Reinforced Composites Using a Robust Stochastic Sampling Approach

Alessandro Polla*
Politecnico di Torino, Turin, 10129, Italy
RMIT University, Melbourne, Victoria, 3000, Melbourne

Riccardo Piani†, Giacomo Frulla ‡ and Enrico Cestino§
Politecnico di Torino, c.so Duca degli Abruzzi 24, Turin, 10129, Italy

Raj Das ¶ and Pier Marzocca ‖
RMIT University, Melbourne, Victoria, 3000, Melbourne

Composite materials are known for their excellent mechanical and light weight properties. However, their vulnerability to interlaminar damages poses a significant challenge for the design of safe and lightweight aerospace structures. Advanced Finite Element Analysis tools based on Cohesive Zone Method and Continuum Damage Mechanics offer a new prospective to investigate impact and damage scenarios to aid the design of structures while paying attention to damage initiation and propagation. A physical-based stacked shell-cohesive modeling technique was implemented in this study to conduct a stochastic analysis of a standardized ASTM composite panel subjected to a blunt high-velocity impact. A comprehensive structured Monte Carlo Latin Hypercube method was applied to quantify uncertainties in interlaminar fracture toughness distribution and to investigate their impact on delamination size and projectile's residual velocity. The results indicate that while resultant global delamination size and shape is less sensitive to material uncertainties, residual projectile's velocity is significantly affected, emphasizing the importance of structured stochastic methods in analysing uncertainty propagation in macro-scale physical-based numerical models subjected to impact or fracture phenomena.

Nomenclature

UQ	=	Uncertainty Quantification
$MC-SRS$	=	Monte Carlo Simple Random Sampling
$MC-LHS$	=	Monte Carlo Latin Hypercube Sampling
CDF	=	Cumulative Distribution Function
COV	=	Coefficient of Variation
$UB-LB$	=	Upper and Lower confidence level Boundaries
G_C	=	Material Fracture Toughness
G_{IC}	=	Mode I interlaminar material fracture toughness
G_{IIC}	=	Mode II interlaminar material fracture toughness
CDM	=	Continuum Damage Mechanics
CZM	=	Cohesive Zone Method
HVI	=	High Velocity Impact

*PhD Candidate, Department of Mechanical and Aerospace Engineering (DIMEAS), AIAA Member, email: alessandro.polla@polito.it
†MSc Candidate, Department of Mechanical and Aerospace Engineering (DIMEAS)
‡Associate Professor, Department of Mechanical and Aerospace Engineering (DIMEAS)
§Associate Professor, Department of Mechanical and Aerospace Engineering (DIMEAS)
¶Professor, Aerospace Engineering and Aviation Discipline
‖Professor and Director, Sir Lawrence Wackett Aerospace Research Centre, AIAA Associate Fellow

$PDFA$	=	Progressive Damage Failure Analysis
SPC	=	Single Point Constraints
E_{CZM}	=	Cohesive interlaminar stiffness
σ_i	=	Cohesive interlaminar strength
$\delta_{e,f}$	=	Cohesive elastic and erosion displacement
$ERODS$	=	Maximum effective strain for element layer failure

I. Introduction

The application of composite materials in the aerospace industry is rapidly increasing. Aerospace composite structures are renowned for their outstanding mechanical performances and lightweight characteristics. Nevertheless, composites are susceptible and incline to interlaminar damages when exposed to low and high-velocity impacts due to the brittle nature of the resin-matrix constituent. Delaminations and back-face failure are a couple of examples of barely visible impact damages observed experimentally [1–3]. Designing safe and lightweight structures with high interlaminar and intralaminar material and structural toughness characteristics poses a significant challenge for the next generation of aircraft.

Advanced Finite Element Analysis (FEA) tools based on Cohesive Zone Method (CZM) [4–6] and Continuum Damage Mechanics (CDM) [7, 8] are now available to model the inter- and intra-laminar region of composite structures. The capabilities of these numerical techniques set the possibility to study and design structure with attention to the damage initiation and propagation at micro- [9, 10] and macro-scale [11] levels. The definition of a robust advanced physical based computational methodology is a key factor to reduce the design and certification process timeline for new composite materials used in future aircraft structures. Physical-based numerical models provide an efficient approach not only for evaluating specific load scenarios but also for assessing uncertainty quantification and conducting statistical material and structural analyses [12]. This allows for the exploration of different material and design variables, enhancing the robustness of structural design analyses.

Physical experiments are still necessary for establishing the mechanical properties of specific structures and material configurations. Standardized experimental procedures are classically employed to determine the stiffness and strength of constitutive materials in various configurations, such as tensile, compression and shear. Additionally, recent modelling techniques, as previously introduced, request the definition of energetic properties related to both inter-laminar and intra-laminar material domains. Since standardized fracture toughness test methods are still not available for all the required properties, the relative material mechanical quantities are significantly affected by uncertainties. Various experimental programs have illustrated the inherent variability in measuring material toughness [13, 14] through experimental procedure currently available in literature. The uncertainty arise from variations in the adopted experimental techniques, manufacturing process, loading conditions, and constitutive sample geometry or characteristics. The statistical uncertainties described can impact the design outcomes and the performance characteristics of an aerospace structure.

Developing a comprehensive understanding of the influence of uncertainties in the generation of experimental material data is time and cost-consuming. Consequently, a conservative approach is commonly adopted to account for these uncertainties. All introduced geometric and material mechanical properties are currently essential in specified numerical models to characterize the mechanical behaviour of each sub-domain within a structure. Despite this, specified quantities are often used as source to generate deterministic input values for computational models. When the same computational architecture is employed to solve the numerical solution, the definition of deterministic inputs leads to deterministic numerical outputs. Therefore, achieving agreement between the deterministic results of a numerical model and the validation results of an experimental campaign can be challenging to justify and accept. The evaluation of model results becomes feasible when stochastic input parameters are also considered in the numerical model's solution, and an efficient Uncertainty Quantification (UQ) analysis is conducted. Characteristic material quantities, such as intralaminar and interlaminar material toughness in carbon fiber reinforced polymers (CFRP) structures, are typically employed to establish design allowances for analytical or computational CZM and CDM models. Enhancing our comprehension of how uncertainty variables interact and propagates during the fracture initiation and propagation in composite structures under non-linear extreme load configurations is crucial.

In this article, a physical-based stacked shell-cohesive modelling technique described in [15] has been adopted to perform a robust stochastic analysis of a standardized ASTM composite panel subjected to a high velocity impact. The analysis is based on experimental results obtained through the Advanced Composite Project (ACP), a collaborative research effort between NASA and FAA [16–18]. The aim of this research is to quantify the propagation of selected

uncertainties in various aspects, including the extension and morphology of delaminations in the post-impact area and the residual impact velocity of a standardized ASTM D8101 impactor [19] following one of the methodology proposed by Pouresmaeeli et al. [20]. The solution is investigated using a Monte Carlo uncertainty quantification methodology. In particular, to obtain an optimized interlaminar fracture toughness distribution for the selected material, a Latin Hypercube Sampling (LHS) methodology has been introduced and implemented. Comparative assessments, both quantitative and qualitative, are conducted on a representative statistical population, and the propagation of uncertainties in the macroscopic numerical results is thoroughly examined and discussed.

The article is organized as follows. Section II delineates the probabilistic uncertainty quantification method selected for this study and introduces the relative probability distribution characteristics selected to describe the material's mechanical properties. The numerical model employed in this analysis and the cited experimental resources adopted in this evaluation are presented in Section III. Subsequently, in Section VI, the probabilistic behaviour observed through the propagation of uncertainties is explicated and discussed. To conclude, a summary of the specified methodology and the established numerical results observed in the article is provided.

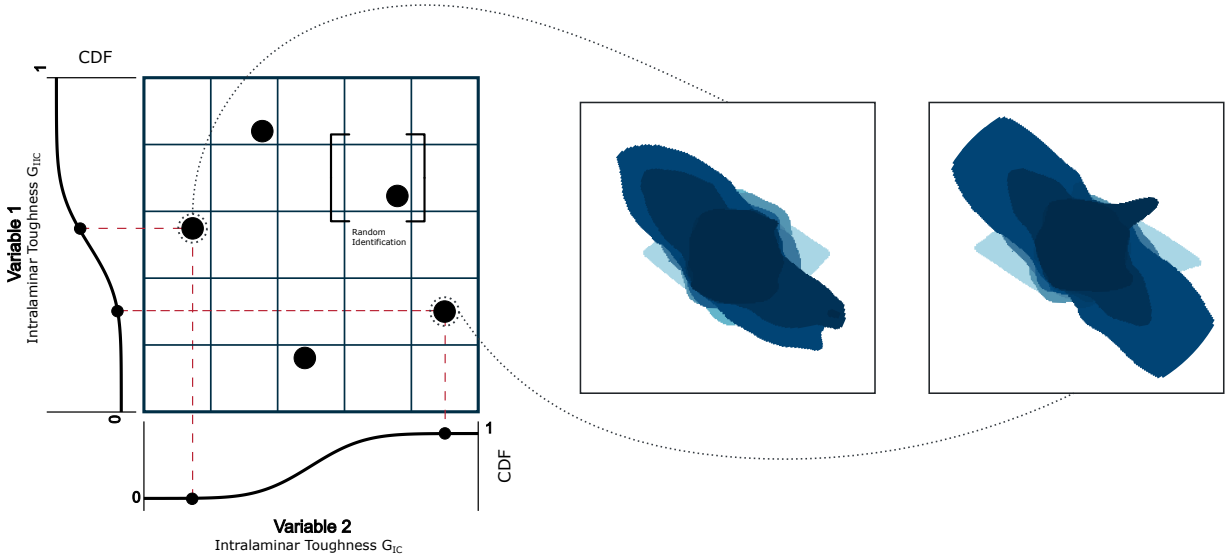

Fig. 1 Conceptual representation of a Monte Carlo Latin Hypercube Sampling (MC-LHS) uncertainty quantification method applied to a High velocity Impact model: representation of the projected post-impact delamination characteristic of two sampled points in a reduced family distribution size. Each sample point is given a specific set of interlaminar toughness values (I, II) based on introduced probability distributions.

II. Probabilistic Analysis Methods

The initiation and propagation of a fracture in fiber-reinforced composite materials is an highly localized phenomena, based on the meso-scale interaction of defects (both pre-existing and generated) with the two constitutive material phases: fiber and matrix. The macro-mechanical energy threshold linked to the meso-scale fracture propagation is commonly quantified through the definition of the characteristic energy release rate (G_c).

In this analysis, the source of uncertainty is identified within the mode-dependent interlaminar fracture toughness of the matrix interface. A structured UQ method has been applied to define the degree of uncertainty reflected in characteristic output associated with impacted composite structures. Monte Carlo Simple Random Sampling (MC-SRS) is considered one of the most versatile uncertainty quantification methodology. However, the method is considered unbiased and memory-less, contributing significantly to the slow convergence time of a given solution [21]. To accurately represent the actual input probability distribution the sampling set of a MC-SRS must comprise a substantial number of individual components. The increasing demand for computationally efficient techniques shifted the focus to the development of the Latin Hypercube Sampling (LHS) uncertainty quantification method. The Monte Carlo Latin Hypercube Sampling can replicate the input distribution using fewer samples compared to the SRS methodology. The

stratification of the input probability distribution based on the Latin square concept leads to more realistic populations and in an increased statistical characteristic coverage of the specified variable domains.
In this context, a two dimensional statistical problem can be represented as a probabilistic square grid. The rows correspond to the Coefficient of Variation (COV) of the first statistical quantity, while the columns are linked to the second variable. The specific problem is considered a Latin Square only when there is precisely one sample within each defined probabilistic interval. Thus, the cumulative curve distribution related with the characteristic input variables is divided into n intervals, each with an equal probability of generation. The two dimensional square grid generated contains n^2 positions that can be filled with only n individual samples Figure 1.

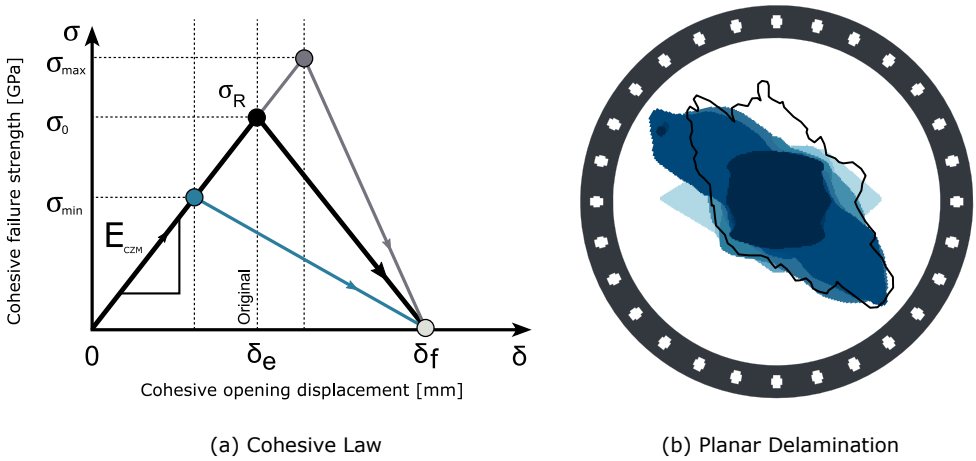

Fig. 2 Interlaminar domain and its representation: (a) Variation of constitutive cohesive stress-displacement relation analysed in the presented analysis; (b) Quantitative comparison of numerical delamination and experimental HVI analysis [22].

The level of uncertainty reflected in damage propagation and energy absorption of the numerical panel have been evaluated. The extension and morphology of delamination were compared in conjunction with the residual velocity of the impactor for different size of populations. A main population of one hundred samples has been selected to investigate the statistical solution with the introduced MC-LHS method. However, based on the Latin cube definition the specified population has been progressively under-sampled to study the convergence of the solution and the accuracy with a reduced number of samples.
Interlaminar fracture surfaces are classically modelled in FE models with the application of a Cohesive Zone Method (CZM). A bilinear traction-separation relation is typically adopted to describe the fibre reinforced composite region that exists within two adjacent adherent composite plies [23, 24]. The relation defines an elastic undamaged phase and a post-failure degradation phase. The cohesive domain is well-defined by the definition of three main material properties: undamaged cohesive stiffness (E_{CZM}), material failure threshold (σ_R), and mode-dependent energy release rate (G_c). The cohesive stiffness, which definition is based on characteristic material properties and selected modelling technique, was considered constant for the described set of analysis. Instead, the interlminar fracture toughness and cohesive strength were assumed to be linearly correlated as described in Figure 2-(a). Consequently, for the same erosion opening displacement (δ_f), a variation of the interlminar fracture toughness leads to a specific variation of the cohesive strength threshold. To quantify propagated uncertainties, the scattering of interlaminar fracture toughness is represented for both pure mode I and mode II as a Gaussian distribution function [25]. The statistical input values of interlaminar mode-dependent fracture toughness were generated using a sampling distribution that is not correlated between the two characteristic variables. The Mode-I cohesive characteristic toughness is scattered with a Coefficient of Variation (COV) of 22.7%, as reported in the experimental data presented in [25]. Similarly, the associated experimental interlaminar Mode-II varies with a COV of 9.3% [25]. The goal of the current analysis is to investigate the potentialities of a MC-LHS UQ technique in estimating characteristic output Cumulative Distribution Functions (CDF) of a HVI computed with a physical based numerical model when the interlaminar toughness is affected by uncertainties.

III. Macro-scale and Interlaminar Damage Model

A High-fidelity shell-cohesive progressive damage failure analysis (PDFA) method has been proposed to numerically reconstruct the performances of a sample subjected to high-velocity impact. A complete stacked shell modelling technique, as described in Polla et al. [15, 26, 27] has been applied including the material models available in the LS-DYNA software package. A square unidirectional T800/F3900 composite panel with 16-ply in a quasi-isotropic layup configuration $[(0/90/45/-45)_2]_S$ has been modelled, as described in [15]. The panel has planar dimensions of 305 × 305 mm and a global thickness of 3.1 mm according to ASTM D8101 standard. A standardized ASTM rigid impactor has been applied. The total mass of the rigid projectile is 50 g with a diameter of 50 mm. A cylindrical clamping section with an internal radius of 127 mm and an external radius of 153 mm has been modelled by single-point constraints (SPC). Homogeneous erosion criteria (ERODS) have been chosen for the deletion of FE elements inside the composite panel [15, 22]. A single plane of 2D shell elements positioned at the relative physical mid-surface is defined for each composite ply belonging to the selected laminate. Interlaminar CZM elements (Cohesive Zone Model) guarantee structural continuity through the thickness being properly connected node-to-node to the adjacent ply mesh structure of each composite layers. Experimental test and material interlaminar and intralaminar mechanical properties for the selected CFRP have been derived from NASA Advanced Composite Project [12, 28, 29] and summarized in [15]. The characteristic mesh size of 1 mm for the composite panel has been selected to satisfy the smeared cracking concept as proposed by Bažant et al. [30]. A structured solid hexa mesh has been applied to the numerical model with a mesh size of 0.5 mm. The accuracy of the numerical model has been verified in [15] by comparing the obtained results with the experimental delamination (Figure 2-(b)) and residual projectile kinematic energy. Numerical simulations are performed using LS-DYNA R11.1.0 explicit single-precision MPP architecture solver, utilizing two nodes on an HPC architecture, each equipped with 12 cores per CPU.

IV. Probabilistic behaviour of high speed impact

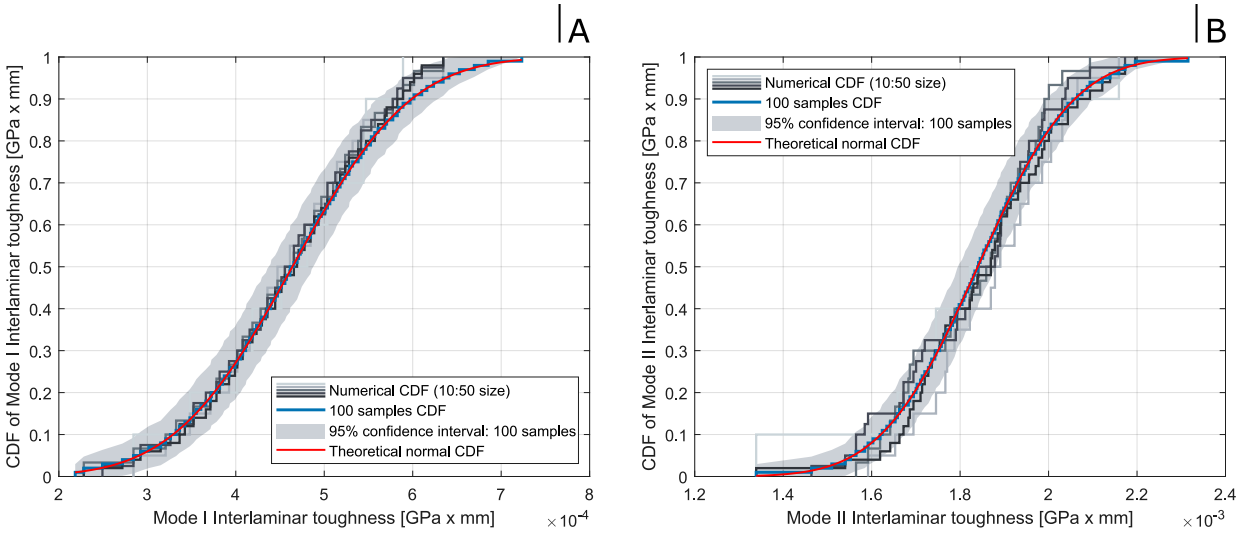

Fig. 3 Discretized interlaminar mode-dependent cohesive toughness probability distributions for different population sizes discretized through the application of MC-LHS uncertainty method: (A) Mode I interaminar toughness distribution; (B) Mode-II interlaminar toughness distribution.

Khaled et al. [29] carried out an experimental test campaign to assess the deterministic mean mode-dependent interlaminar material toughness of selected T800/F3900 composite material. Analytical Gaussian distribution of specified material properties have been sampled through a Monte Carlo Latin Hypercube Sampling (MC-LHS) approach with variations in population sizes. The resultant input distributions in Figure 3 were considered as uncertainty variables for the introduced problems. All probability distributions satisfy the goodness-fit-test with the theoretical normal distribution function reported in [25].

In Figure 4 the convergence of the solution for different population sizes is illustrated on a logarithmic scale. A satisfactory convergence of the mean value for the delamination extension can be observed. The absolute convergence

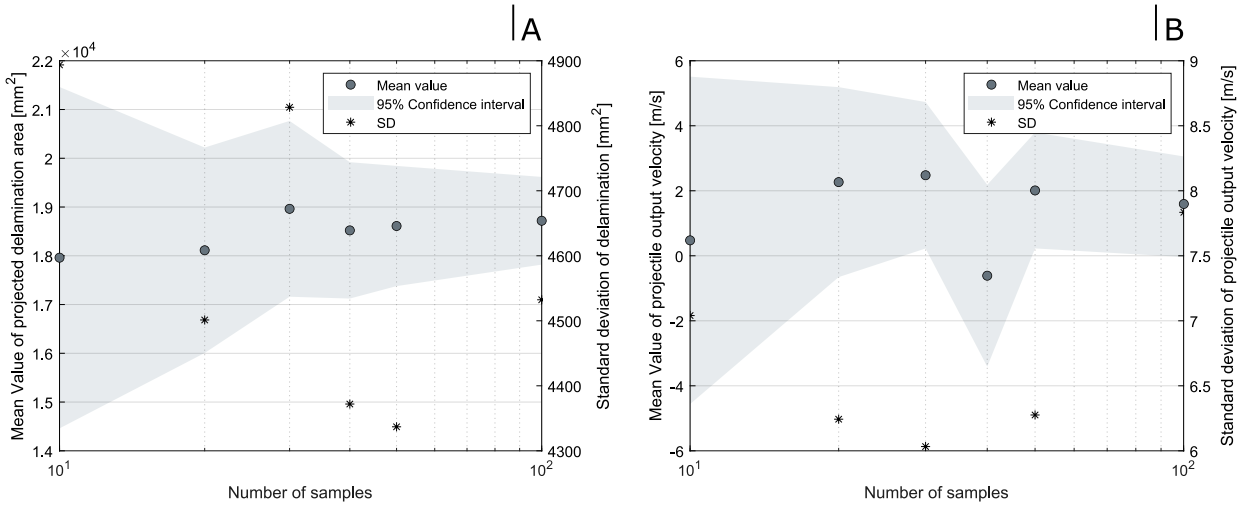

Fig. 4 Convergence of the mean and standard deviation value of uncertainty outputs: (A) projected delamination extension; (B) residual projectile velocity.

Variable	Delamination (mm^2) - [$x10^4$]					
Population	N = 10	N = 20	N = 30	N = 40	N = 50	N = 100
Mean	1.796	1.811	1.896	1.852	1.861	1.871
95% CI for Mean: LB	1.446	1.6	1.716	1.712	1.738	1.782
95% CI for Mean: UB	2.146	2.022	2.076	1.992	1.984	1.962
Median	1.671	1.837	1.882	1.836	1.864	1.866
Std. Deviation	0.489	0.45	0.482	0.437	0.434	0.453
Variable	Statistical Moments					
Population	N = 10	N = 20	N = 30	N = 40	N = 50	N = 100
Skewness	0.761	0.144	0.625	0.370	0.557	0.409
Kurtosis	2.535	2.388	3.405	2.878	3.589	2.995
P-value (Null Hp)	NaN	NaN	0.392	0.272	0.244	0.549

Table 1 Statistical quantities of projected delamination extension in HVI test using the MC-LHS.

of the projectile velocity is less consistent with the variation of the population size. Based on the reduced number of sample in the populations the convergence of both standard deviation values is slow ($O(1/N)$) if compared with the mean behaviour($O(1/\sqrt{N})$. This observed slow convergence of the standard deviation values is characteristic when a solution is obtained through Monte Carlo UQ family methods [31]. The mean distribution for the projected delamination area can be assumed consistent for each family group. The delamination size is observed varying in a range of $1.8 - 1.9\, x10^4$ mm^2. Residual impact velocity of the projectile oscillates with increasing population size but stabilizes and assume the value of 1.5m/s for the population of 100 samples.

The convergence value do not match with the experimental result and the validated prediction of the numerical model described in [15]. This discrepancy can be attributed to the utilization of a distinct computational architecture for the current methodology compared to the one proposed in [15].

The variation of specific numerical results based on the selected multi-node computational architecture configuration used to solve the input model have been already described in literature and cited in the software user manual [32, 33]. However, taking into consideration this constrain the phenomenology can be evaluated to quantify the propagation of uncertainties and the statistical distribution of specified outputs based on the input property definitions. A consistent convergence of interval of confidence for both characteristic parameters is observed. Statistical moments related with defined population sizes analysed in this study are presented in Table 1 and Table 2. Table 1 displays the mean and

Variable	Projectile Velocity (m/s)					
Population	N = 10	N = 20	N = 30	N = 40	N = 50	N = 100
Mean	0.475	2.266	2.478	-0.613	2.01	1.509
95% CI for Mean: LB	-4.561	-0.656	0.225	-3.411	0.227	-0.038
95% CI for Mean: UB	5.511	5.188	4.731	2.184	3.793	3.057
Median	0.297	2.608	2.853	1.353	2.931	2.56
Std. Deviation	7.04	6.243	6.032	8.746	6.275	7.8
Variable	Statistical Moments					
Population	N = 10	N = 20	N = 30	N = 40	N = 50	N = 100
Skewness	-0.575	-0.658	-0.495	-0.842	-1.277	-0.882
Kurtosis	3.246	3.841	3.279	3.279	6.337	4.026
P-value (Null Hp)	NaN	NaN	NaN	0.155	0.132	0.139

Table 2 Statistical quantities of absolute projectile velocity extension in HVI test using the MC-LHS.

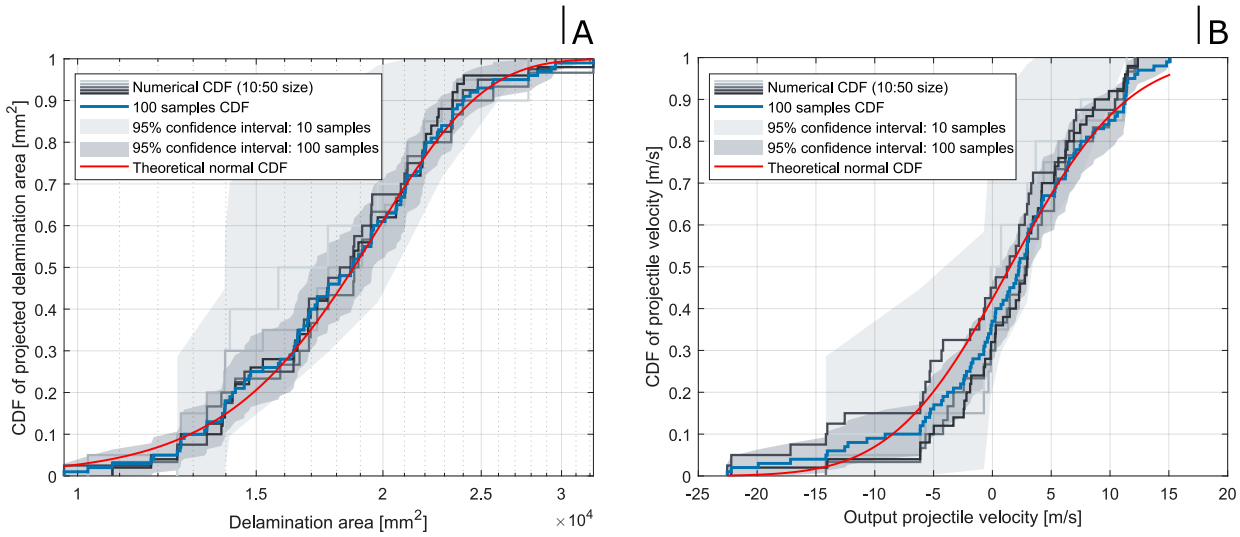

Fig. 5 CDFs for different population size with the minimum and maximum confidence interval: (A) projected delamination area; (B) residual projectile velocity.

standard deviation associated with the delamination size, evaluated across an increased number of samples. An oscillatory behaviour is evident for both Skewness and Kurtosis values, stabilizing at approximately 0.4 and 3, respectively. Consequently, delamination size distribution exhibits longer tails in the third quartile and a moderately peaked function for the impacted CFRP panels. The probability distribution can be characterized as light-tailed and symmetrical. A Goodness of Fit test reveals a P-value exceeding 0.05, thereby validating the null hypothesis. On the other hand, the observed behaviour in Figure 3 - B for the residual projectile velocity can be thoroughly examined in Table 2. With a Skewness value of -0.882 for the larger family group, the distribution of the projectile output velocity exhibits a longer tail in the first quartile. In addition, a Kurtosis value exceeding 3 indicates a probability distribution with thick tails. A higher number of samples is required to assess the Goodness of Fit factor for the specific distribution. The probabilistic distribution of the projectile's residual velocity can be described as approximately normal, as verified by the null hypothesis, with thick and long left tail. This behaviour underscores the distribution's tendency to align with the observed -7.70 m/s experimental results from NASA [22]. Figure 5 A and B represents the Cumulative Distributions Functions (CDF) of specified output quantities. The observations defined through the evaluation of characteristic statistical moments can be visually appreciated in the reported CDF. Delamination's distribution can clearly define a central normal distribution with reduced confidence interval with an higher number of samples. CDF relative to the projectile

residual velocity shows longer tail on the left side of the distribution. The output CDFs here proposed are only a couple of example of statistical evaluations that can be used to compare the experimental results obtained with the numerical solution when a model is affected by a statistical variation of one or multiple material constitutive mechanical properties. Even if physical-based numerical modelling techniques are implemented, the stochastic micro and meso scale fibre-matrix interaction of each tested structure can not be correctly evaluated without a structured statistical analysis. Previous findings have relied on assessing the projected delamination size through the evaluation of a MC-LHS method with different population sizes. The projected delamination is an experimental output commonly defined through C-Scan analysis to assess the interlaminar delamination observed in an impacted structure. However, the projected delamination size does not precisely represent the localized extension of the damage within an impacted composite structure. Typically, each interlaminar layer exhibits a distinct delamination size that can not easily discerned through C-Scan analysis.

The radar plot depicted in Figure 6 illustrates the delamination size associated with each ply-to-ply interlaminar section. Each point belonging to represented curve sets the relative ply-to-ply delamination size obtained through the corresponding numerical simulation. The extent of damage observed in each interlaminar region was normalized relative to the ply-to-ply interlaminar delamination observed in the reference simulation conducted with the numerical model validated in [15]. This normalization allows for a precise definition of the extension and morphology of the entire delamination defined by the specific simulations. In both examples depicted in Figure 6, the majority of interlaminar delaminations attain the same size as the benchmark reference. However, delaminations occurring between plies 3-4 and 7-8 show higher variations compared to the reference values. Interlaminar regions 3-4 and 7-8 represent domains enclosed within two adjacent unidirectional (UD) plies oriented at 90 degrees respectively each other. These regions are particularly sensitive to damage initiation and propagation in CFRP. The relative values shown in Figure 6 indicate that only a few ply-to-ply interlaminar regions exhibit delamination size different than the reference model, such as observed in the interlaminar region between plys 3-4 or 7-8.

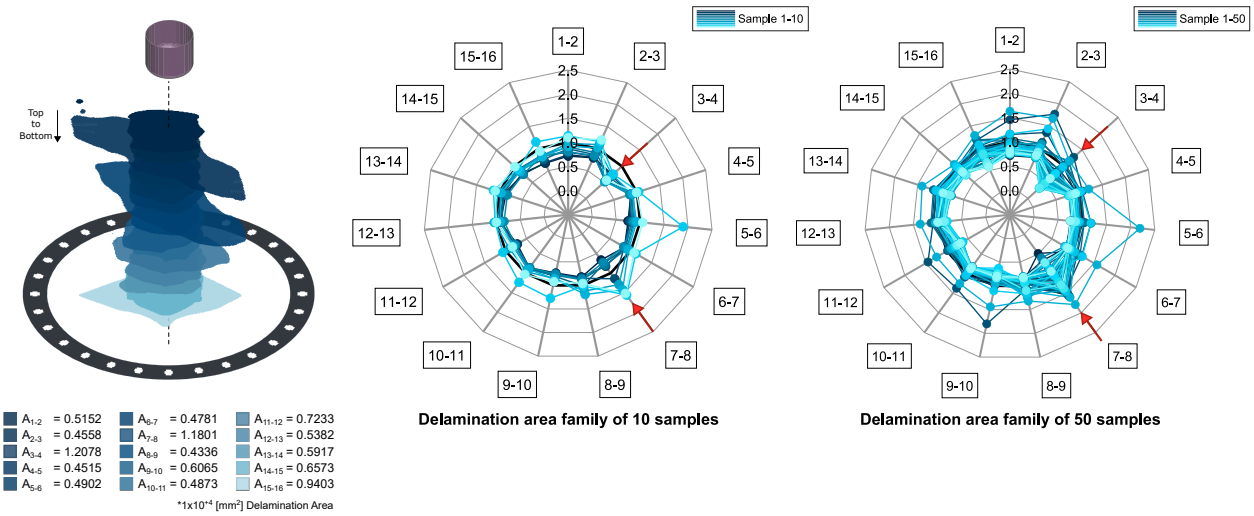

Fig. 6 Interlaminar ply-to-ply delamination size for two representative families relative to the validated delamination size.

V. Conclusion

The present study introduced a comprehensive stochastic analysis for examining interlaminar fracture in a composite panel subjected to high-velocity impact loads using a standardized ASTM circular-flat projectile. To address these computationally expensive problems, a robust and efficient uncertainty quantification technique based on a Monte-Carlo Latin Hypercube was applied to a macro-scale numerical model to study and verify the uncertainties propagation associated with a statistical variation of two characteristic interlaminar mechanical material properties (G_{IC} and G_{IIC}).

Specifically, the interlaminar mode-dependent fracture toughness, representing the characteristic material fracture properties, was considered as a source of uncertainty for assessing the impact evolution. Statistical output distribution associated with the delamination size and residual ASTM impactor velocity have been reconstructed for each population sizes investigated. The convergence analysis of specific output variables involved monitoring the evolution of mean values and standard deviations unique to each population size. Statistical moments were also examined to measure the shape of the numerical distributions in comparison to the analytical normal distribution. In conclusion, the extension of the projected impact delamination can be associated with a standard Gaussian distribution. The results shows that a reduced number of samples is adequate to assess the mean delamination size value linked with characteristic impact conditions but with a large confidence interval. On the other hand, the probability distribution of the residual projectile velocity can be associated with a normal distribution but with thicker and longer tail in the first quartile. A bigger population size is mandatory to observe a converged standard deviation value for both the observed numerical quantities due to the convergence characteristic of this specific quantity in a MC method. Statistical analysis revealed that degree of uncertainty in selected numerical input propagate through a variation of the residual projectile's velocity in comparison with the delamination size. The macroscopic projected shape and extension of the interlaminar delamination seems less sensitive to material input uncertainties than the projectile residual velocity. The research reveals how structured stochastic methods can be used efficiently to analyse uncertainty propagation in macro-scale numerical model subjected to impact or fracture phenomena.

Acknowledgments

We gratefully acknowledge the support and provision of computational resources by HPC@POLITO, a project of Academic Computing within the Department of Control and Computer Engineering at the Politecnico di Torino. The HPC PoliTo cluster played a crucial role in enabling the resolution of the numerical models associated with the specific research. We sincerely appreciate the invaluable assistance provided by HPC@POLITO, which will significantly contribute to the successful completion of our study.

References

[1] Tan, W., Falzon, B. G., Chiu, L. N., and Price, M., "Predicting low velocity impact damage and Compression-After-Impact (CAI) behaviour of composite laminates," *Composites Part A: Applied Science and Manufacturing*, Vol. 71, 2015, pp. 212–226. https://doi.org/10.1016/j.compositesa.2015.01.025.

[2] González, E., Maimí, P., Martín-Santos, E., Soto, A., Cruz, P., Martín de la Escalera, F., and Sainz de Aja, J., "Simulating drop-weight impact and compression after impact tests on composite laminates using conventional shell finite elements," *International Journal of Solids and Structures*, Vol. 144-145, 2018, pp. 230–247. https://doi.org/10.1016/j.ijsolstr.2018.05.005.

[3] Soto, A., González, E., Maimí, P., Mayugo, J., Pasquali, P., and Camanho, P., "A methodology to simulate low velocity impact and compression after impact in large composite stiffened panels," *Composite Structures*, Vol. 204, 2018, pp. 223–238. https://doi.org/10.1016/j.compstruct.2018.07.081.

[4] Dugdale, D., "Yielding of steel sheets containing slits," *Journal of the Mechanics and Physics of Solids*, Vol. 8, No. 2, 1960, pp. 100–104. https://doi.org/10.1016/0022-5096(60)90013-2.

[5] Barenblatt, G., "The Mathematical Theory of Equilibrium Cracks in Brittle Fracture," *Advances in Applied Mechanics*, Vol. 7, Elsevier, 1962, pp. 55–129. https://doi.org/10.1016/S0065-2156(08)70121-2.

[6] Tvergaard, V., and Hutchinson, J. W., "The relation between crack growth resistance and fracture process parameters in elastic-plastic solids," *Journal of the Mechanics and Physics of Solids*, Vol. 40, No. 6, 1992, pp. 1377–1397. https://doi.org/10.1016/0022-5096(92)90020-3.

[7] Matzenmiller, A., Lubliner, J., and Taylor, R., "A constitutive model for anisotropic damage in fiber-composites," *Mechanics of Materials*, Vol. 20, No. 2, 1905, pp. 125–152. https://doi.org/10.1016/0167-6636(94)00053-0.

[8] Donadon, M. V., Iannucci, L., Falzon, B. G., Hodgkinson, J. M., and Almeida, S. F. M. d., "A progressive failure model for composite laminates subjected to low velocity impact damage," *Computers & Structures*, Vol. 86, No. 11, 2008, pp. 1232–1252. https://doi.org/https://doi.org/10.1016/j.compstruc.2007.11.004.

[9] Varandas, L. F., Catalanotti, G., Melro, A. R., Tavares, R. P., and Falzon, B. G., "Micromechanical modelling of the longitudinal compressive and tensile failure of unidirectional composites: The effect of fibre misalignment introduced via a stochastic process," Vol. 203, 2020. https://doi.org/https://doi.org/10.1016/j.ijsolstr.2020.07.022.

[10] Varandas, L. F., Catalanotti, G., Melro, A. R., and Falzon, B. G., "On the importance of nesting considerations for accurate computational damage modelling in 2D woven composite materials," Vol. 172, 2020, p. 109323. https://doi.org/https://doi.org/10.1016/j.commatsci.2019.109323.

[11] Furtado, C., Catalanotti, G., Arteiro, A., Gray, P. J., Wardle, B. L., and Camanho, P. P., "Simulation of failure in laminated polymer composites: Building-block validation," Vol. 226, 2019, p. 111168. https://doi.org/https://doi.org/10.1016/j.compstruct.2019.111168.

[12] Hoffarth, C., Khaled, B., Shyamsunder, L., and Rajan, S. D., "Development of a Tabulated Material Model for Composite Material Failure, MAT213: Part 1: Theory, Implementation, Verification & Validation," , No. DOT/FAA/TC-19/50, P1, 2020.

[13] Brunner, A. J., Blackman, B. R. K., and Williams, J. G., "Calculating a damage parameter and bridging stress from GIC delamination tests on fibre composites," *Composites Science and Technology*, Vol. 66, No. 6, 2006, pp. 785–795. https://doi.org/https://doi.org/10.1016/j.compscitech.2004.12.040.

[14] Wang, W.-X., Nakata, M., Takao, Y., and Matsubara, T., "Experimental investigation on test methods for mode II interlaminar fracture testing of carbon fiber reinforced composites," *Composites Part A: Applied Science and Manufacturing*, Vol. 40, No. 9, 2009, pp. 1447–1455. https://doi.org/https://doi.org/10.1016/j.compositesa.2009.04.029.

[15] Polla, A., Frulla, G., Cestino, E., Das, R., and Marzocca, P., "Coupled Thermo-Mechanical Numerical Modeling of CFRP Panel under High-Velocity Impact," *Aerospace*, Vol. 10, No. 4, 2023, p. 367. https://doi.org/10.3390/aerospace10040367.

[16] Byar, A. D., Pang, J. K., Iqbal, J., Ko, J., and Rassaian, M., "Determination of Ballistic Limit for IM7/8552 Using LS-DYNA," *AIAA SciTech Forum*, 2018, p. 11.

[17] Hunziker, K. J., Pang, J., Pereira, M., Melis, M., and Rassaian, M., "NASA ACC High Energy Dynamic Impact Methodology and Outcomes," *2018 AIAA/ASCE/AHS/ASC Structures, Structural Dynamics, and Materials Conference*, American Institute of Aeronautics and Astronautics, 2018. https://doi.org/10.2514/6.2018-1700.

[18] Justusson, B., Pang, J., Molitor, M., Rassaian, M., and Rosman, R., "An Overview of the NASA Advanced Composites Consortium High Energy Dynamic Impact Phase II Technical Path," *AIAA Scitech 2019 Forum*, American Institute of Aeronautics and Astronautics, 2019. https://doi.org/10.2514/6.2019-2052.

[19] Committee, D., "Test Method for Measuring the Penetration Resistance of Composite Materials to Impact by a Blunt Projectile," Tech. rep., ASTM International, 2017. https://doi.org/10.1520/D8101_D8101M-18.

[20] Pouresmaeeli, S., and Falzon, B., "Uncertainty quantification of pure and mixed mode interlaminar fracture of fibre-reinforced composites via a stochastic reduced order model," *Composite Structures*, Vol. 278, 2021. https://doi.org/10.1016/j.compstruct.2021.114683, URL https://linkinghub.elsevier.com/retrieve/pii/S0263822321011399.

[21] Sudret, B., Marelli, S., and Wiart, J., "Surrogate models for uncertainty quantification: An overview," *2017 11th European Conference on Antennas and Propagation, EUCAP 2017*, 2017, p. 793 – 797. https://doi.org/10.23919/EuCAP.2017.7928679.

[22] Shyamsunder, L., Maurya, A., Rajan, S. D., Cordasco, D., Revilock, D., and Blankenhorn, G., "Impact simulation of composite panels for aerospace applications," *Composites Part B: Engineering*, Vol. 247, 2022. https://doi.org/10.1016/j.compositesb.2022.110320.

[23] Turon, A., Camanho, P. P., Costa, J., and Dávila, C. G., "A damage model for the simulation of delamination in advanced composites under variable-mode loading," *Mechanics of Materials*, Vol. 38, No. 11, 2006, pp. 1072–1089. https://doi.org/https://doi.org/10.1016/j.mechmat.2005.10.003.

[24] Turon, A., Camanho, P. P., Soto, A., and González, E. V., "Analysis of Delamination Damage in Composite Structures Using Cohesive Elements," *Comprehensive Composite Materials II*, Elsevier, 2018, pp. 136–156. https://doi.org/10.1016/B978-0-12-803581-8.10059-1.

[25] Crews, J. H., and Reeder, J. R., "A mixed-mode bending apparatus for delamination testing," *Nasa Technical Memorandum 100662*, 1988.

[26] Polla, A., Piana, P., Cestino, E., and Frulla, G., "Delamination and Fracture Modeling Techniques for Shell Composite Structures in LS-DYNA®," 2021.

[27] Polla, A., Frulla, G., Cestino, E., Das, R., and Marzocca, P., "A Structured Methodology to Simulate Composite Advanced Joint Behavior for Ultra-Light Platforms Applications," *Applied Sciences*, Vol. 13, No. 2, 2023, p. 1004. https://doi.org/10.3390/app13021004.

[28] "Development of a Tabulated Material Model for Composite Material Failure, MAT213 Part 2: Experimental Tests to Characterize the Behavior and Properties of T800-F3900 Toray Composite," , No. DOT/FAA/TC-19/50, P2, 2019.

[29] Khaled, B. M., Shyamsunder, L., Holt, N., Hoover, C. G., Rajan, S. D., and Blankenhorn, G., "Enhancing the predictive capabilities of a composite plasticity model using cohesive zone modeling," *Composites Part A: Applied Science and Manufacturing*, Vol. 121, 2019. https://doi.org/10.1016/j.compositesa.2019.03.001.

[30] Bažant, Z. P., and Oh, B. H., "Crack band theory for fracture of concrete," *Matériaux et Constructions*, Vol. 16, No. 3, 1983, pp. 155–177. https://doi.org/10.1007/BF02486267.

[31] Borello, F., Cestino, E., and Frulla, G., "Structural Uncertainty Effect on Classical Wing Flutter Characteristics," *Journal of Aerospace Engineering*, Vol. 23, No. 4, 2010-10, pp. 327–338. https://doi.org/10.1061/(ASCE)AS.1943-5525.0000049.

[32] TECHNOLOGY, L. S., *LS-DYNA® KEYWORD USER'S MANUAL, VOLUME I, LS-DYNA R13*, Vol. I, 2021. URL www.lstc.com.

[33] TECHNOLOGY, L. S., *LS-DYNA® KEYWORD USER'S MANUAL, VOLUME II, LS-DYNA R13*, Vol. II, 2021. URL www.lstc.com.